

OLD YELLOW ENZYMES: HIGHLY HOMOLOGOUS FMN-OXIDOREDUCTASES WITH MODULATING ROLES IN OXIDATIVE STRESS AND PROGRAMMED CELL DEATH IN YEAST
Osama Odat¹, Samer Matta¹, Hadi Khalil¹, Sotirios C. Kampranis¹, Raymond Pfau², Philip N. Tsiachlis², Antonios M. Makris¹

From the ¹Department of Natural Products, Mediterranean Agronomic Institute of Chania, P.O. Box 85, Chania 73100, Greece, and ²Molecular Oncology Research Institute, 750 Washington Street, Tufts-NEMC Box 5609, Boston, MA 02111

Running title: OYE in oxidative stress and PCD

O.O, S.M. & H.K contributed equally.

Address correspondence to: Antonios M. Makris, Department of Natural Products, Mediterranean Agronomic Institute of Chania, Alysillon Agrokepiou, Chania 73100, Greece. Tel.: 30-28210-35050; Fax: 30-28210-35001; e-mail: antoniosmakris@yahoo.gr

In a genetic screen to identify modifiers of Bax-dependent lethality in yeast, the C-terminus of OYE2 was isolated based on its capacity to restore sensitivity to a Bax-resistant yeast mutant strain. Overexpression of full length OYE2 suppresses Bax lethality in yeast, lowers endogenous reactive oxygen species (ROS), increases resistance to H₂O₂-induced programmed cell death (PCD) and significantly lowers ROS levels generated by organic prooxidants. Reciprocally, *Δoye2* yeast strains are sensitive to prooxidant-induced PCD. Overexpression and knockout analysis indicates these OYE2 antioxidant activities are opposed by OYE3, a highly homologous heterodimerizing protein, which functions as a prooxidant promoting H₂O₂-induced PCD in wild type yeast. To exert its effect OYE3 requires the presence of OYE2. Deletion of the 12 C-terminal amino acids and catalytic inactivation of OYE2 by a Y197F mutation enhance significantly survival upon H₂O₂-induced PCD in wild type cells, but accelerate PCD in *Δoye3* cells, implicating the *oye2p-oye3p* heterodimer for promoting cell death upon oxidative stress. Unexpectedly, a strain with a double knockout of these genes (*Δoye2 oye3*) is highly resistant to H₂O₂-induced PCD, exhibits increased respiratory capacity, and undergoes less cell death during the adaptive response in chronological aging. Simultaneous deletion of OYE2 and other antioxidant genes hyperinduces endogenous levels of ROS, promoting H₂O₂-induced cell death: in *Δoye2 glr1* yeast high levels of oxidized glutathione elicited gross morphological aberrations involving the actin cytoskeleton, and defects in organelle partitioning. Altering the ratio of

reduced to oxidized glutathione by exogenous addition of GSH fully reversed these alterations. Based on this work, OYE proteins are firmly placed in the signaling network connecting ROS generation, PCD modulation and cytoskeletal dynamics in yeast.

Cell suicide responses regulated through programmed cell death (PCD) have been documented not only in higher organisms but also in bacteria and in yeast. In nature, unicellular organisms exist as populations in an environment with limited resources (1); thus a conserved suicide program in which older or damaged cells sacrifice themselves and release nutrients to the remaining cells promotes continued group survival (2-4). Cell death with apoptotic features has been reported in yeast treated with low concentrations of acetic acid or hydrogen peroxide (5,6), with DNA damage induced by UV radiation treatment (7), after exposure to high levels of mating pheromone (8), and upon aging (9). Recently, it has become clear that a core PCD machinery exists in *S. cerevisiae*. For example, yeast with mutations in the CDC48 gene, an AAA family member involved in the fusion of ER-derived vesicles (10), exhibit characteristic hallmarks of apoptotic cell death including DNA fragmentation, chromatin remodelling (11), and annexin V staining (12). Similarly, expression of a mutant form of the mammalian ortholog of CDC48, valosin containing protein (VCP), induces mammalian cells to undergo apoptosis (13). Yeast analogs of a number of components of the canonical apoptotic machinery have been described. Yeast homologs for caspase-like proteases, YCA1 (14); for the OMI/HtrA2 protease, NMA111 (YNL123w) (15); for Apoptosis

Inducing Factor (AIF), YNR074C; and for AIF-homologous mitochondrion-associated inducer of death (AMID), NDI1, have all been implicated in the regulation of PCD in yeast (16,17).

Heterologous expression of mammalian regulators of apoptosis in yeast can influence yeast PCD. Expression of the anti-apoptotic protein Bcl-2 can rescue a superoxide dismutase (SOD)-deficient yeast strain (18), whereas expression of the pro-apoptotic counterpart Bax or Bak kills yeast in a manner that resembles PCD induced by these proteins in mammalian cells. Upon expression in yeast, Bax localizes mainly in the mitochondria and promotes mitochondrial membrane hyperpolarization (19), causing an eventual collapse of $\Delta\Psi_m$ and release of Reactive Oxygen Species (ROS) and cytochrome c. This phenotype has been exploited to isolate proteins inhibiting Bax lethality (20), allowing the identification of BI-1, a highly conserved apoptosis inhibitor (21), enzymes involved in the ROS detoxification such as BI-GST (22) and ascorbate peroxidase (23), and Ku70, an evolutionarily conserved component of the dsDNA repair machinery (24).

Previous work in our lab isolated a series of EMS-mutagenized yeast strains that exhibited resistance to Bax-induced PCD (25). To further exploit the effect of Bax and obtain insights on the yeast PCD machinery, we have here utilized one such mutant that failed to target Bax to mitochondria, in a reverse genetic screen to identify yeast proteins that restore sensitivity to Bax. This screen identified the C-terminus of the conserved flavin mononucleotide (FMN) oxidoreductase OYE2. Suggestively, the highly related OYE3 protein, which is known to heterodimerize with OYE2 (26), had previously been found to modulate Bax-dependent PCD in yeast (27).

In the current study, we show that full length OYE2 suppressed Bax lethality in wild type yeast, and is a potent antioxidant protein. This activity contrasts with that of OYE3, which antagonized the protective action of OYE2 in H₂O₂-induced programmed cell death. The effect of OYE3 requires the presence of OYE2, indicating that it is the oye2p-oye3p heterodimer that facilitates PCD. Surprisingly, the absence of both genes rendered cells hyper-resistant to H₂O₂-induced PCD by increasing their respiratory efficiency. Deletion of OYE2 with other antioxidant genes elevated endogenous ROS and sensitized cells further to H₂O₂-induced PCD. In the case of *oye2 glr1* cells, the cellular redox environment

with high levels of oxidised glutathione led to gross morphological aberrations, actin cytoskeleton abnormalities and defects in organelle partition between mother and daughter cells. Together, these results indicate that OYE2 is a connection point between ROS generation, modulation of PCD, and cytoskeletal regulation.

Experimental Procedures

Genetic screen in yeast - A previously characterised EMS mutagenised yeast strain R13 (*his3 ura3 trp1 LexA-operator-LEU2*) carrying the pGILDA/Bax plasmid was transformed with a yeast genomic library on the plasmid pJG4-5(25). Growing colonies were replica plated on Glucose/CM-his, trp and galactose-raffinose/CM-his, trp. Colonies growing on glucose media but not on galactose, where Bax is expressed, were selected for further characterization. The library plasmids were extracted and then reintroduced into fresh cells and were tested for the reproducibility of the Bax resensitization phenotype. The library plasmids capable of restoring Bax lethality were sequenced.

Growth recovery curves - Fresh overnight cultures of the various yeast strains grown in Glu/CM media or glucose media lacking the amino acid used as auxotrophic marker were washed with dH₂O and resuspended in fresh medium at OD₆₀₀=0.1. Aliquots were taken at regular intervals and the absorbance was measured. When the OD₆₀₀>1, the aliquots were serially diluted and new measurements were taken. To examine the effect of a transient pulse of H₂O₂ in cultures overexpressing the OYE proteins, fresh cells were resuspended at OD₆₀₀=0.1 in fresh glucose media and 2 hours later, at the end of the lag period, the cultures were supplemented with 1.5 or 1.25 mM H₂O₂ and were incubated with shaking at 30°C. The ability of the cell populations to recover from the H₂O₂ insult was assessed by measuring growth at OD₆₀₀ at regular intervals. All growth recovery assays were performed independently in triplicate.

Plasmid constructs- The full lengths of the OYE2 and OYE3 genes were PCR amplified from wild type yeast genomic DNA using the primers 5'-OYE2(EcoRI) 5'-GAA TTC ATG CCA TTT GTT AAG GAC TTT AAG CC-3' and 3'-OYE2(XhoI) 5'-CTC GAG TTA ATT TTT GTC CCA ACC GAG TTT TAG-3' for OYE2 and 5'-OYE3-CAA TTG ATG CCA TTT GTA AAA GGT TTT GAG CCG ATC-3' and 3'-OYE3 5'-CTC GAG TCA GTT CTT GTT CCA ACC TAA ATC

TACT GC-3' OYE3. A fusion of the OYE2 with GFP in the C-terminus was prepared using a two-step PCR approach with overlapping primers. In the first step, OYE2 was amplified using the primer 5'OYE2(EcoRI) and 3'OYE2(GFP) 5'-CTC GCC CTT GCT CAC ATT TTT GTC CCA ACC-3' and the GFP construct was amplified using the 5'OYE-GFP 5'-GGT TGG GAC AAA AAT GTG AGC AAG GGC GAC-3' and the 3'GFP(XhoI) 5'-CTC GAG TTA CTT GTA CAG CTC GTC CAT GCC-3'. The amplified products from the first round were gel extracted and purified. A small aliquot of the two fragments was mixed in a new PCR reaction using the 5'OYE2(EcoRI) and the 3'GFP(XhoI) external primers. All PCR amplifications were made using Platinum Taq polymerase (Invitrogen). The purified fragments were cloned into the pCR2.1 TOPO TA vector according to the manufacturer's instructions. All the cloned inserts were subsequently subcloned into the yeast expression vectors: pJG4-6, expressing the proteins under a galactose promoter; and pYX143 and pYX143-HA (hemagglutinin tagged), which are low copy number vectors (*ARS/CEN*, *LEU2*) expressing the genes under the control of the constitutive TPI promoter. Expression of the proteins was verified in the pYX143-HA and pJG4-6 in western blots using antibodies against the HA tag. BY4741 wild type yeast cells were transformed with pYX143-OYE2, pYX143-OYE3, or a control empty plasmid. Protein expression was verified indirectly by parallel cloning of the OYE2 and OYE3 cDNAs into the pYX143-HA vector, which expresses the cDNAs fused to a hemagglutinin tag. However, the untagged vectors were used in all subsequent experiments to eliminate the possibility of any interference of the HA tag.

A C-terminal truncated construct of OYE2 was generated by PCR using the primer 5'OYE2 and 3'OYE2(1-388) 5'-CTC GAG CTA CGT AGG GTA GTC AAT GTA-3'. The product was sequenced and subcloned into the pYX143-HA and pYX143 vectors. Mutation of tyrosine 197 to phenylalanine in OYE2 was generated according to the directions of QuickChange Site-Directed Mutagenesis protocol from Stratagene. The complementary primers OYE2(Y197F)5 5'-CCA CAG CGC TAA CGG TTT CTT GTT GAA CCA GTT CTT G-3' and OYE2(Y197F)3 3'-CAA GAA CTG GTT CAA CAA GAA ACC GTT AGC GCT GTG G-3' were used in a PCR reaction run for 16 rounds using *Pfu Turbo* DNA polymerase. Subsequent to DpnI digestion of nonmutated

parental DNA, the digest was used to transform bacterial cells. Plasmid DNA from isolated colonies was sequenced to verify the mutation. The Y197F OYE2 cDNA was subcloned into pYX143, pYX143-HA yeast vectors as above.

Flow-cytometric studies. Yeast strains growing in glucose complete media, till late logarithmic phase, were washed with PBS and stained. Dihydroethidium (HE; D-1168, Molecular Probes) at 4 μ M was used as an indicator of endogenous reactive oxygen species (ROS). Yeast cells harbouring plasmids were grown in glucose complete media lacking the amino acid used as the auxotrophic marker. To assess cellular responses to pro-oxidants, aliquots of grown cells were treated for 1 hour with 1.5 mM hydrogen peroxide (H_2O_2), 1 mM *t*-butyl hydroperoxide (*t*-BOOH), or 0.2 mM cumene hydroperoxide (CHP). Subsequent to treatment, cells were washed extensively with PBS by repeated centrifugations and were finally stained with HE as above. Using FACS, 100,000 cells from each sample were measured. Quantification was performed using the Cytomation software (DAKO).

Microscopy and fluorescence measurements - Mitochondrial import and morphology was visualised using the plasmid pVT100U-mitGFP or the plasmid pYX142-mitGFP (which expresses GFP fused to a mitochondrial matrix targeting sequence) which were introduced in yeast cells (28). The organelles were observed in a single plane so as to observe the relative diameter of the tubules. Actin filaments were stained by fixing with 4% formaldehyde and staining using rhodamine-phalloidin (R-415, Molecular Probes). Nuclei were stained with Hoechst 33342. To mask fluorescence from mitochondrial DNA a low dose of Mitotracker Red CMXRos (M7512, Molecular Probes) was used as a counterstain. The lumen of yeast vacuoles was stained with 50 μ M CMAC (Y-7531, Molecular Probes) for 20 min. At the end of incubations cells were washed twice, resuspended in prewarmed PBS, applied on microscope slides and observed under 1000X magnification in a fluorescent microscope. Necrotic cells with permeabilized outer membranes were measured by Evans blue staining. In addition to FACS analysis, ROS were also measured using a Perkin Elmer LS55 Luminescence spectrometer. Fresh cultures of cells were resuspended in PBS at $OD_{600}=0.5$ and 1ml aliquots of cells were stained with Mitotracker Red CMXRos (M-7512, Molecular Probes) for 15 min. in the dark and washed once with PBS at the end of incubation the cells were resuspended in 2 mls and

fluorescence was measured over the optimal emission range.

Generation of double knockout yeast strains - A yeast strain harbouring a deletion of the OYE2 gene was generated by integrating a URA3 cassette originating from the pUG72 plasmid(29). The primers 5'OYE2 lox 5'-TCA TAT TAA GCT AAA TAT AGA CGA TAA TAT AGT ATC GAT AAT GCC ACA GCT GAA GCT TCG TAC GC-3' and 3'OYE2 lox 5'-AAA TGG TGC TAC AAA GTA CGG TTA ACA CTA TTA ATT TTT GTC CCA ACC GCA TAG GCC ACT AGT GGA TCT G-3' which contain flanking sequences from the 5' and 3' of the OYE2 gene were used to amplify the cassette in a PCR reaction. The amplified DNA fragment was purified and was transformed into a Mat alpha strain which originated by repeated backcrosses to a BY4741 background. Proper integration of the URA cassette was verified by PCR using the primers 5'GenOYE2 5'-CAC GAC AAG ATT CTT CTA TTG ATT ATT CAC ATA TGT-3' and 3'OYE2 lox. To generate double knockouts the Δ oye2::URA3 strain was mated to BY4741 deletion strains Δ oye3, Δ sod1, Δ ctl1, Δ glr1, Δ yca1, and Δ gsh1 (Research Genetics) which harbour the G418 antibiotic resistance marker on the deleted gene. Diploid cells were induced to sporulate and the regenerating spores were tested in Glu/CM-ura, +G418 plates. The mating type of the double knockout haploid strains was subsequently assessed.

ρ^0 strains (lacking functional mitochondria) were generated from the ρ^+ Δ oye2 oye3 strain by growing cells in YPD broth containing 10 μ g/ml ethidium bromide for 3 days (30). Dilutions were plated on YPD plates and growing colonies were tested for their capacity to grow on YPGlycerol media.

Induction of PCD with H₂O₂, acetic acid and colony viability assays - Cells growing in logarithmic phase were used to inoculate at very low density in fresh glucose media. A small aliquot was subsequently removed, serially diluted, and plated on rich YPD plates. This represented the 0 timepoint and viability 100%. To the diluted cells, H₂O₂ was added to 1 mM and cells were incubated for 2 hours at 30°C. Treated cells were enumerated as above, and compared to the original count. All experiments were performed independently in triplicate. The presence of necrotic cells was determined by staining with Evans blue and visualisation by light microscopy. Acetic acid induced PCD was performed in accordance to the

protocol described by Ludovico et al (5) using unbuffered Glu/CM media.

Chronological aging assays- All strains were grown in 10 ml cultures with unbuffered glucose complete media (2% glucose) till saturation. At the end of the second day of incubation, a small aliquot of cells was removed and the number of live cells was enumerated by serial dilution and plating on YPD plates. This corresponded to 0 timepoint. Aliquots of cells were removed regularly and cells were enumerated as above.

Determination of Total Glutathione and Glutathione Disulfide. BY4741, Δ oye2, Δ oye3, Δ oye2 oye3 and Δ oye2 glr1 cells were grown till late log phase in Glu/CM. Total glutathione and glutathione disulfide were measured according to a method described by Griffith (31) and modified by Kampranis (22)

Results

The FMN-oxidoreductase OYE2 limits Bax-induced lethality in yeast. To identify yeast genes that participate in PCD processes we took advantage of the Bax-induced lethal phenotype in yeast. The Bax-resistant EMS-mutant strain R13, which exhibits defects in mitochondrial protein targeting (25), was used in a screen to identify yeast proteins which can restore Bax sensitivity. We transformed cells containing a galactose-inducible Bax expression plasmid with a yeast genomic library cloned into the pJG4-5, galactose-inducible, yeast expression vector. Transformed yeast were initially plated on glucose selective plates at low density to enable us to pick distinct colonies. Approximately 3,000 colonies were replica-plated on glucose and galactose selective media to induce Bax and library expression from the galactose promoter.

One of the library clones that converted Bax resistant R13 cells back to sensitivity contained the C-terminus of OYE2 from amino acid 314 to the end of the gene (aa 314-400). The gene is translated from a proximal ATG supplied from the pJG4-5 vector (Fig. 1).

Reekmans *et al* have recently shown that deletion of OYE3, an FMN oxidoreductase homologous to OYE2, attenuated Bax-induced growth arrest, cell death and caused a decrease in NADPH in yeast (27). Among the EMS mutant yeasts we previously generated, that are resistant to Bax-induced PCD, a significant proportion also showed defects in protein transport to mitochondria, most likely limiting integration of Bax to the outer membrane. Expression of (314-400) OYE2 in R13

cells not only sensitized cells to Bax lethality (Fig. 1A), but also restored the ability of GFP fused to a mitochondrial targeting sequence (mit-GFP) to associate with mitochondria (Fig. 1C), indicating that OYE2 can affect mitochondrial targeting. The size of R13 cells also decreased and resembled wild type appearance.

In wild type yeast, Bax causes changes in the morphology of the mitochondria. While in a percentage of cells the organelles become fragmented, the remaining cells exhibit fewer swollen organelles most likely by fusion as a defence response (Fig. 1B). YFP-Bax localized to mitochondria in wild type cells, whereas in the R13 Bax resistant mutant the YFP fusion clearly fails to target the organelles (Fig. 1B bottom row). Co-expression of YFP-Bax with the (314-400) OYE2 C-terminus reversed the diffused fluorescence, however only very weak peripheral fluorescence could be detected (data not shown).

YFP-Bax is lethal to R13 cells, only when co-expressed with the (314-400) OYE2 despite the difficulty to detect its fluorescence. Recently TOM22, a component of the complex responsible for initial import of mitochondrial targeted proteins was identified as a Bax receptor (32). This could explain the frequent association between Bax resistance and defects in mitochondrial protein translocation in our mutants (25).

We next overexpressed the full-length open reading frame of OYE2 from the pJG4-4 vector, under the control of a galactose inducible promoter. In wild type EGY48 cells expressing Bax, overexpression of the full length OYE2 suppressed Bax lethality, whereas the C-terminus OYE2 could not do so (Fig. 2A). OYE2 also reversed to a large extent mitochondrial swelling, as well as excessive mitochondrial fission, both characteristics effects of Bax expression in sensitive yeast strains (Fig. 2B). Full length OYE2 did not resensitize the R13 mutant cells to Bax (data not shown), suggesting that this action of the (314-400) OYE2 represented a dominant negative effect of the truncated protein. Supporting the OYE2 protective role, Bax expression in $\Delta oye2$ was more toxic compared to wild type yeast (data not shown).

OYE2 localizes to mitochondria. As OYE2 was isolated based on restoring Bax-sensitivity to a strain with deficient localization of Bax to its site of action, the mitochondria, we asked if OYE2 might itself associate with mitochondria. A full-length OYE2-GFP fusion was introduced into EGY48 cells

under the control of a galactose-inducible promoter. OYE2-GFP localized to distinct domains in the cytoplasm that partially overlapped with mitochondria (Fig. 2C). This indicates that OYE2 localized on the organelle and can thus limit directly the capacity of Bax to insert and oligomerize on the mitochondrial outer membrane (OM). The OYE2-GFP fusion weakly protected wild type cells from Bax lethality and did not act as dominant negative (data not shown).

OYE2 and OYE3 have opposing functions in regulation of oxidative stress in wild type yeast. Bax-induced lethality in yeast is strongly linked to enhanced intracellular oxidative stress (33). OYE3 modulates Bax-dependent PCD (27), and heterodimerizes with OYE2 *in vivo* and *in vitro* (26). Further, OYE2 and OYE3 share 82% identity at the amino acid level, suggesting a related activity. To elucidate the functional relationship of OYE2, and OYE3, we expressed them at moderate levels in yeast and assessed basal and induced levels of oxidative stress.

Yeast overexpressing OYE2 or OYE3, or vector transformed control cells, were treated with 1.5 mM H₂O₂, with 1 mM of the prooxidant *tert*-butyl hydroperoxide (*t*-BOOH), and with 0.2 mM of the prooxidant cumene hydroperoxide (CHP). After incubation, cells were stained with dihydroethidium (HE) to gauge oxidative stress: Figure 3A compares FACS-determined HE values for cells overexpressing OYE2 or OYE3 (hatched lines) in reference to cells expressing empty vector (vertical lines) for each condition. In untreated cells, overexpression of OYE2 modestly lowered (-13%), and of OYE3 elevated (+24%), endogenous ROS, when compared to wild type BY4741 cells harbouring empty vector. These modest changes were reproducible by FACS and by experiments measuring ROS using a luminescence spectrometer done in triplicate. OYE2 or OYE3 overexpression did not significantly influence ROS levels following treatment with H₂O₂ (-3% and +7% respectively). However, treatment of cells with organic prooxidants generated more dramatic differences in ROS levels dependent on OYE status. Overexpression of OYE2 caused a substantial reduction in ROS levels in both *t*-BOOH (-13%) and CHP (-44%) treated cells compared to their wild type counterparts, suggesting an antioxidant activity. In contrast, overexpression of OYE3 caused a substantial increase in ROS levels, implying a prooxidant activity (+25% for *t*-BOOH and +37% for CHP).

To further analyze OYE function, we performed similar experiments, comparing basal or induced ROS in wild type parental BY4741 yeast with ROS in strains deleted for OYE2 or OYE3 ($\Delta oye2$ and $\Delta oye3$). Both deletion strains showed similar ROS levels under basal conditions, or following H_2O_2 treatment $\Delta oye2$ cells treated with CHP exhibited a small increase in ROS (+12%); whereas $\Delta oye3$ cells showed lower ROS levels upon *t*-BOOH and CHP treatment (-20% and -18% respectively) (Figure 3A). These changes in ROS again suggested antioxidant activity for OYE2, and prooxidant activity for OYE3. The ROS changes upon CHP treatment are more dramatic and tend to show higher heterogeneity as a general feature, which was observed in a large series of deletion strains tested (data not shown). To support these ROS alterations, all experiments with overexpression and deletion strains were also performed using Mitotracker CMXRos staining and detection with a fluorescence spectrometer: identical patterns of variance were seen (data not shown).

To assess the physiological relevance of the changes observed in endogenous ROS levels in our tested strains, we additionally examined $\Delta sod1$ and $\Delta ctt1$ cells harbouring deletions in superoxide dismutase 1 and catalase 1 respectively. $\Delta sod1$ cells exhibited elevated endogenous ROS (+52%) compared to parental BY4741 wt cells. Treatment with H_2O_2 led to an additional increase in ROS (+69%). In contrast, no changes in ROS levels were seen in treated or untreated $\Delta ctt1$ cells (Fig. 3B).

OYE2 and OYE3 have opposing functions in the regulation of PCD. Under standard growth conditions, the growth of yeast overexpressing OYE2 or OYE3 is undistinguishable from that of control cells (not shown). We next asked if OYE status regulated cell viability and sensitivity to PCD induced by different stimuli. H_2O_2 is a standard inducer of PCD in yeast (6); we examined cellular viability of H_2O_2 -treated yeast cells overexpressing OYE2 or OYE3. Strikingly, cells overexpressing OYE2 recovered more rapidly than did control cells, entering log phase at 12 versus 22 hours following H_2O_2 addition, while cells overexpressing OYE3 failed to recover even at 40 hours after treatment (Fig. 4A). Given the effect of the C-terminus of OYE2 on the R13 mutant, we also tested a 12 amino acid truncated form (1-388) of OYE2. This short stretch of sequence was relatively unstructured, as revealed by the crystal structure information. Cells overexpressing (1-388) OYE2

were compared to cells overexpressing OYE2 or empty vector treated with H_2O_2 . Overexpression of the truncated construct resulted in even higher numbers of surviving cells, indicating an important role for the C-terminal region of OYE2 in PCD modulation (Fig. 4B).

Complementing this assay, independent experiments were performed by pulsing diluted cells with H_2O_2 for 2 hours and subsequently plating on YPD plates to allow determination of colony forming units (CFU; Figure 4C). Overexpression of OYE2 led to a small increase in viability ($P < 0.0001$), while overexpression of OYE3 caused a decrease in viability compared to wild type cells. The modest drop in viability of the OYE3 overexpressing cells ($P = 0.007$) can be attributed to the transient pulse of H_2O_2 in the assay. Overexpression of (1-388) OYE2 elevated substantially the number of viable cells as in the previous assay. Treatment with H_2O_2 and subsequent staining of cells with Evans blue did not show any increase in necrotic cells in any of the cultures (not shown), confirming that loss of viability was not due to necrosis.

To assess whether the death promoting capacity of OYE3 requires the presence of OYE2 and possibly formation of heterodimers, OYE3 was overexpressed in $\Delta oye2$ cells harbouring a deletion for the OYE2 gene. OYE3 homodimers in $\Delta oye2$ cells exert a protective function (Fig. 4D). Inversely overexpression of OYE2 in $\Delta oye3$ cells maintained its protective function. However, overexpression of (1-388) OYE2 offered no protection in $\Delta oye3$ cells, indicating that the protective effect of the C-terminal truncation is exerted upon heterodimerization to OYE3 (Fig. 4E). Additionally, we tested a point mutation of OYE2 in which tyrosine 197 (Y196 in *S. pastorianus* OYE) is changed to a phenylalanine, previously shown to cause a dramatic decrease of its oxidative half-reaction but to have little effect on ligand binding and its reductive half-reaction (34). Overexpression of Y197F OYE2 in BY4741 wild type cells caused an important increase in cell viability upon H_2O_2 -induced PCD (Fig. 4G) as in the case of C-terminal truncation. To assess whether the effect of Y197F OYE2 is exerted on the heterodimer with OYE3, we overexpressed the mutant protein in $\Delta oye3$ cells (Fig. 4H). Whereas overexpression of OYE2, that is OYE2 homodimers, were protective in H_2O_2 -induced PCD, expression of the Y197F OYE2 in $\Delta oye3$ cells was

lethal and cells were unable to recover after 30 hours incubation.

Taken together, our data indicate that formation of oye2p-oye3p heterodimers contributes to the induction of PCD upon oxidative stress, and that obstruction of heterodimer formation in wild type cells by co-expressing (1-388) OYE2 or Y197F OYE2 leads to elevated survival.

Double deletion of OYE2 and OYE3 renders cells highly resistant to H₂O₂-induced PCD. Extending further on the overexpression results, we analyzed cell death induced by a H₂O₂ pulse in Δ oye2, Δ oye3, and Δ oye2 oye3 (double knockout) yeast, versus the BY4741 parental control. In liquid medium, Δ oye3 cells recovered more quickly than wild type cells and Δ oye2 more slowly than wild type cells (Figure 5A), reciprocal to the results seen with overexpression (Figure 4A). Unexpectedly, the Δ oye2 oye3 double knockout yeast recovered earlier than all the other strains. These recovery results coincide with the independent colony viability assays of cells pulsed with H₂O₂ for 2 hours (Fig. 5B). Δ oye2 cells were more susceptible to H₂O₂-induced PCD than wild type cells, whereas Δ oye3 cells were more resistant. Again, Δ oye2 oye3 cells were highly resistant to H₂O₂, maintaining >50% viability under conditions where BY4741 cells were only 8% viable. The magnitude of protection of Δ oye2 oye3 cells was assessed by comparison to Δ yca1 a deletion strain in the apoptotic yeast metacaspase. Cells treated with lower H₂O₂ dose (0.8 mM) were monitored in growth survival assays. Δ yca1 cells at this concentration performed only slightly better than wild type cells, whereas Δ oye2 oye3 cells were markedly better off than both strains (Fig. 5C). The extent of survival differences was further enhanced at higher H₂O₂ concentrations (1.25-1.5 mM) (not shown). Staining of H₂O₂ treated cells with annexin V/ Evans blue showed increased PS externalization, one of the hallmarks of apoptosis (Fig. 5D). Annexin stained cells did not internalize Evans blue dye, confirming the apoptotic nature of death.

The endogenous ROS levels of Δ oye2 oye3 were nearly identical to wild type cells (Fig. 5E). Overexpression of OYE2, OYE3 or (1-388) OYE2 in Δ oye2 oye3 cells reduced in all cases survival upon H₂O₂ treatment (Fig 5F).

We next compared the relative respiratory capacity of OYE deletion strains, since increases in respiratory rates are frequently escorted with adaptation of the cell antioxidant machinery to cope with increased toxic byproducts of respiration. To

assess respiratory capacity, serial dilutions of yeast were plated in parallel on rich medium (YP) with glucose (YPD) or glycerol (YPG) as carbon sources. EGY48 was an efficiently respiring positive control, while parental BY4741 cells had a more limited respiratory capacity. Although deletion of single OYE genes had little effect, Δ oye2 oye3 cells exhibited growth on glycerol equivalent to the EGY48 cells, and significantly higher than the single knockouts and the BY4741 parental strain (Figure 5G). Deletion of both OYE caused a qualitative change in cellular physiology that enhanced respiration, which probably triggered an adaptive response from the antioxidant machinery that effectively kept ROS at low levels.

To examine whether active respiration in Δ oye2 oye3 is important for resistance to cell death from oxidative stress, we proceeded to generate ρ^0 strains (lacking functional respiration) from the isogenic Δ oye2 oye3 strain. Cells were treated with ethidium bromide to eliminate mitochondrial DNA (30). Five colonies were tested in parallel to Δ oye2 oye3 cells by plating serial dilutions on YPDextrose and YPGlycerol plates to verify the absence of respiration (Fig. 5H). All tested strains were confirmed to be ρ^0 . Three ρ^0 Δ oye2 oye3 strains were selected and pulsed with H₂O₂ for 2 hours and colony viability was enumerated by plating on YPD plates (Fig. 5I). All 3 ρ^0 Δ oye2 oye3 strains were sensitive to H₂O₂-induced PCD. Growth recovery curves, performed in parallel, exhibited identical sensitivities (not shown), but was not the assay of choice due to growth difference between untreated ρ^+ and ρ^0 strains. Overall, our data underline the importance of respiration in resistance to PCD from oxidative damage.

Response of Δ oye2 oye3 to aging and acetic acid induced cell death. In cultures growing in high glucose levels, an age- and pH- dependent form of programmed cell death occurs, in which the majority of the cells die and eventually an adapted subpopulation emerges in their place (34). To assess this form of PCD wild type BY4741, Δ oye2, Δ oye3 and Δ oye2 oye3 cells were grown in 10 ml cultures in glucose complete media (2% glucose) until saturation. At the end of the second day of incubation, a small aliquot of cells was removed and the number of live cells was enumerated by serial dilution and plating on YPD plates. This corresponded to 0 timepoint. Aliquots of cells were removed regularly and cells were enumerated as above. The Δ oye2 oye3 cells exhibited reproducibly a substantial decrease in the percentage of dying

cells during the adaptive regrowth process (Fig. 5J). The reduced cell death during chronological aging could be explained by the physiological changes that have taken place in the DKO strain, as evidenced by their increased respiratory capacity. This induced form of cell death is known to be associated with nutrient, pH, and the redox status of the yeast strain. In the long run though (>15 days) the viable cell counts were always lower than wild type cells.

Finally, acetic acid also induces PCD and increases levels of ROS in yeast (5). We therefore proceeded to examine the potential involvement of OYE2 and OYE3 in this type of cell death, using experimental regimens similar to those used for H₂O₂. BY4741, *Δoye2*, *Δoye3* and *Δoye2 oye3* yeast were grown to logarithmic phase, then aliquots of cells were treated with increasing concentrations of acetic acid (10, 20, 40 mM), and used for colony forming assays (Figure 5K). The percentage of necrotic cells was estimated by staining treated cells with a non-permeant Evans blue dye, and was found to be comparable to non-treated cells for all cases (1-3%). At the lowest concentration of 10 mM acetic acid, the parental cells exhibited a minimal reduction of cell viability around 20%. The reduction of viability was proportional to the increasing concentrations of acetic acid. The rate of viability loss was equivalent for all strains at each concentration time point, suggesting that acetic acid induced PCD may utilize a distinct mechanism from H₂O₂-induced PCD.

Double inactivation of oye2 with other antioxidant genes increases ROS and H₂O₂-induced PCD. The preceding data indicate OYE2 regulates intracellular redox conditions. To further explore this idea, we combined deletion of OYE2 with deletion of additional redox control genes. The strains *Δsod1*, *Δctl1*, *Δyca1*, *Δglr1* (GLR1 encodes a cytosolic and mitochondrial glutathione oxidoreductase that converts oxidized glutathione to reduced glutathione, a critical cellular antioxidant) (35,36) and their double knockout counterparts' *Δoye2 sod1*, *Δoye2 ctl1*, *Δoye2 yca1*, and *Δoye2 glr1* were grown to late logarithmic phase in glucose complete media were stained with HE to measure ROS and were analyzed by FACS, as above. Additionally, the ability of single and double knockout strains to recover from H₂O₂ treatment was examined in growth recovery assays (Fig. 6). Comparison of ROS levels between wild type BY4741 cells and the single knockouts *Δsod1*, *Δctl1* (shown in Figure 3B) *Δyca1* and *Δglr1* (Fig. 6)

showed increased ROS only in the case of *Δsod1* (Fig. 3B). When their double knockout counterparts with *oye2* were compared to the single knockouts, in all cases besides *Δoye2 ctl1* they exhibited substantial increases in ROS levels, confirming further the role of OYE2 as an antioxidant gene since deletion of the gene further exacerbates the endogenous oxidative environment in cells harboring deletions in antioxidant genes. A series of 20 additional single and double mutants to other known antioxidant genes were also tested with the same results (A.M., unpublished data). Furthermore, examination of the sensitivity to H₂O₂-induced PCD of single and DKO, *Δsod1* and *Δoye2 sod1* (Fig. 6, top row), *Δyca1* and *Δoye2 yca1* (Fig. 6, third row), *Δglr1* and *Δoye2 glr1* (Fig. 6, bottom row) showed increased sensitivity to H₂O₂-induced PCD in the double knockouts compared to the single knockouts or wild type cells.

Double inactivation of oye2 with glr1 increases morphological defects. Intriguingly, microscopic observations of the *Δoye2 glr1* strain revealed gross morphological abnormalities of the emerging buds. Examination of the *Δoye2 glr1* mitochondria, by expressing mit-GFP from a pYX142 plasmid, showed thinner than normal organelle mitochondrial tubules, indicating excessive fragmentation (Fig. 6) (37). A role for OYE2 in the protection of actin from oxidative damage was recently proposed (38); based on such a role, defects in actin skeleton dynamics might lead to altered trafficking of Bax to mitochondria, or failure to accurately organize mitochondria.

To assess the role of inactivation of *oye2* and *glr1* on the actin cytoskeleton and intracellular organelles, we stained wild type, *Δoye2*, *Δglr1*, and *Δoye2 glr1* strains with rhodamine-conjugated phalloidin to visualize actin, with Hoechst 33342 to detect nuclei, and with CMAC to visualize vacuolar lumens (Figure 7). *Δoye2* cells resembled the wild type cells in actin stain, though overall they appeared to stain more intensely actin patches (Fig. 7). The same pattern was also observed in the DKO *Δoye2 oye3* cells, although the cells were overall larger in size. Deletion of GLR1 caused a noticeable increase in actin cable staining, but also a decrease in actin patches. In the *Δoye2 glr1* strain there were dramatic aberrations in cell morphology, with cells containing large hyperelongated buds. There was excessive stain of actin cables decorating in a dispersed manner throughout the whole cell. The cells are not pseudohyphal as they are haploid. These suggest a failure in the cells to properly

control polarized cell growth. The actin cytoskeleton changes for $\Delta oye2$ cells seen by Haarer and co-workers in the FY23x86 genetic background were not observable in BY4741 cells used in the large scale gene deletion project (Research Genetics), as shown in figure 7. The appearance of the $\Delta oye2 glr1$ cells resembles the extreme phenotype of the actin mutant *act1-123* (R68A, E72A) (38).

Many organelle segregation events utilize actin cables for polarized transport. Nuclei stained with Hoechst revealed that a large number of the hyperelongated buds are lacking a nucleus in the $\Delta oye2 glr1$ cells, likely caused by failure to partition the organelle. A significant proportion of the hyperelongated buds, during active growth phase, spontaneously died as shown by their permeability to the Evans blue stain. However, vacuoles partitioned successfully between mother and daughter cell, although the daughter vacuoles localized at the very tip of the elongated bud, giving it a very characteristic appearance (Fig. 7).

Addition of exogenous GSH restores cell morphology in $\Delta oye2 glr1$ cells. The cytoskeletal and morphological aberrations are specific to the double inactivation of OYE2 and GLR1, since a double knockout $\Delta oye2 gsh1$ (GSH1 catalyses the first step in glutathione biosynthesis), although it contains very high levels of endogenous ROS, and is very sensitive to oxidative stress, it does not assume the aberrant cytoskeletal morphology (Fig. 8). This suggests a special role for GSSG in combination with *oye2p* in the regulation of actin polymerization. To assess GSH and GSSG levels late log phase cultures from BY4741 wt cells, $\Delta oye2$, $\Delta oye3$, $\Delta oye2 oye3$, and $\Delta oye2 glr1$ cells were treated as described (22). GSH levels are significantly lower only in $\Delta oye2$ cells ($P < 0.0001$), whereas in GSSG there is a striking 6-fold increase in the $\Delta oye2 glr1$ cells. To further validate the importance of GSSG, we attempted to reverse the GSH/GSSG ratio in the cells, by exogenously supplementing media with 5 mM GSH. As seen in Fig. 8, supplementation with GSH completely reversed the aberrant morphology of the $\Delta oye2 glr1$ cells. These results confirm the participation of oxidized glutathione together with the absence of *oye2* in eliciting actin cytoskeletal changes.

DISCUSSION

A significant proportion of the EMS-mutant yeast strains that are resistant to Bax lethality exhibit

additional aberrations in mitochondrial morphology and defects in proper targeting of a mit-GFP to the mitochondrial matrix (25% of strains) (25). This close association is supported by the recent identification of TOM22, a component of the outer mitochondrial membrane import complex (TOM) as a mitochondrial receptor of Bax (32). In the R13 strain currently examined, Bax failed to localize to mitochondria enabling cells to survive. The presence of the C-terminus of OYE2 restored Bax sensitivity and additionally enabled proper mit-GFP targeting. Mutations in the mitochondrial import complex (including TOM22) and actin cytoskeleton dependent transport are known to cause disruptions in mitochondrial morphogenesis (39).

The Old Yellow Enzyme of yeast was the first flavoprotein to be discovered, in 1932. OYE was initially purified from *S. carlsbergensis* (*oye1p*), and later from *S. cerevisiae* (*oye2p* and *oye3p*). Old yellow enzymes form homodimers, but can also form heterodimers of 45kDa subunits with one monovalently bound FMN per subunit. The enzyme is rapidly reduced by NADPH and can be reoxidised by oxygen. Both OYE proteins have been shown to catalyze the NADPH-dependent reduction of quinones and of several α and β unsaturated carbonyl compounds (26,40). To date, few studies have addressed the physiological relation of the two *S. cerevisiae* OYE.

The use of heterologous proteins Bax and Bak in yeast pointed early on to the involvement of mitochondria and oxidative stress in eliciting cell death (19,22,41). Although there have been many doubts raised with regard to the necessity of the presence of a conserved suicide program in unicellular organisms, several studies in the past few years uncovered yeast apoptotic components that are direct counterparts of the standard mammalian apoptosis regulators. In the current study we show that the two OYE proteins modulate oxidative stress and the propensity of cells to undergo H_2O_2 -induced apoptosis. The *oye2p* and *oye3p* proteins exert an opposing effect in oxidative stress in wild type cells. The *oye2p* protein clearly maintains a protective antioxidant role; efficiently removing ROS generated from organic prooxidants while the *oye3p* protein enhances ROS levels under the same conditions. The study of H_2O_2 -induced PCD in overexpression and deletion strains confirmed these activities and identified the *oye3-oye2* heterodimer as being responsible for the enhanced sensitivity to H_2O_2 -induced PCD. The *oye2p* is an important participant in the antioxidant

machinery, as its simultaneous deletion with other antioxidant genes exacerbates oxidative stress (Fig. 6).

OYE2 and OYE3 share extensive homology (82% identity). Construction of molecular models of OYE2 and OYE3 based on the structure of OYE from *S. pastorianus* (42) reveals that the vast majority of changes are found on surface exposed regions of the two proteins and appear to result in significant alterations on the surface charge, which could have a profound effect on the protein interaction specificities of the two isoenzymes. Information compiled in public protein interaction databases such as Biogrid has identified different protein partners for OYE2 and OYE3 (43-46). In the vicinity of the active site all residues that are found in the crystal structure of *S. Pastorianus* OYE to be interacting with FMN are conserved. Only one substitution is observed in the surface binding cavity. F297 of OYE2 is substituted with S in OYE3. The residues could play an important role in the substrate specificity of the enzymes and should be addressed in future experiments (Fig. S1 and S2). Experimental examination of catalytic stereospecificity of OYE2 and OYE3 using α,β -unsaturated carbonyl compounds identified differences between them (47). *In vivo* assays of yeast cells exposed to the toxic α,β -unsaturated carbonyl acrolein, a product of lipid peroxidation in biological systems, identified OYE2 but not OYE3 for its contribution to acrolein tolerance (48). Our data show that in addition to catalytic specialization and differential protein binding, the stoichiometry of the oye2p-oye3p heterodimer to homodimers is important for the propensity of the cells to undergo cell death upon oxidative trigger. The catalytic activity of OYE2 is important for the function of the complex, as seen by the inactivating mutation at Y197 of OYE2. The C-terminus of OYE2 is also shown to participate in PCD modulation. A 12 amino acid truncation at the C-terminus of OYE2 substantially elevated the protection levels conferred in H₂O₂-induced apoptosis. A larger fragment of the C-terminus restored Bax sensitivity and proper mitochondrial targeting in the R13 mutants. Interestingly the C-terminus of OYE2 was also identified as the site of interaction with actin. Mutation of the 3 terminal amino acids in OYE2 abolished this binding (38). Overexpression of the Y197F OYE2 mutant exhibited the same protective response as the truncated OYE2 protein in wild type cells but was lethal in H₂O₂ insulted cells lacking OYE3 pointing that the protective effects of the

altered proteins were due to the obstruction of the oye2p-oye3p heterodimer. The integrity of the core apoptotic machinery appears important for the death promoting effects of oye3p-oye2p since deletion in apoptosis inducers abolished the induction of cell death caused by OYE3 overexpression (data not shown).

Transcriptional control of the OYE genes may play a key role in determining the formation of homodimers versus heterodimers in the cells. Data from microarray studies indicate that the two OYE genes are not co-regulated. Computational approaches for inferring sets of regulatory modules (sets of co-regulated genes which are controlled by a shared regulatory program) assigns the two genes in different modules. OYE3 clusters into a mitochondrial module that is under the control of BCY1, the cAMP-dependent protein kinase regulatory subunit, whereas OYE2 clusters into a diverse group enriched in enzymes (includes GSH2, GLR1, TRR1) under the control of UME1, the negative regulator of meiosis. OYE2 expression is substantially reduced when cells enter stationary phase, but no such drastic change is seen for OYE3 (49,50). Thus, differential regulation of the two genes could modulate sensitivity to PCD at various stages in their life cycle.

Deletion of both OYE genes brought about a qualitative change in the cells, elevating respiratory activity, which led to their increased resistance to PCD as well as the reduction of cell death during senescence prior to adaptive regrowth. Incapacitation of respiration in the $\Delta oye2 oye3$ cells diminished their resistance to cell death from oxidative damage. The importance of functional mitochondria in resistance to oxidative stress has been known for some time (51). Apoptosis caused by expression of the yeast AMID homologue NdiI, can be repressed by increased respiration on glucose-limited media (17). The changes in resistance to H₂O₂ seen in $\Delta oye2 oye3$ cells are not caused by elevated ROS levels upon increased respiration, since those are identical to the parental wild type cells. Grant and co-workers postulated that the role of mitochondrial function in resistance may depend in some energy requiring process (51) which remains to be identified.

A first biological function of OYE2 was recently uncovered by Haarer and co-workers (38). Flexibility in the C-terminus of yeast actin, and the red blood cell actin, allows two cysteine residues (Cys374 and Cys285) to come into proximity, and in a sufficiently oxidizing environment form a

disulfide bond. In human cells, actin undergoes glutathionylation of Cys374 during cell adhesion, and impairment of actin glutathionylation inhibits the disassembly of the actinomyosin complex (52). The *oye2* protein, but not the *oye3* protein, was shown to interact with actin possibly in the proximity of the Cys285-Cys374 disulfide bond (38). A nearly complete knockdown (37-388) of OYE2 crossed to *oye3Δ* strain was used by Haarer *et al.* to show defects in cytoskeletal organization, with excessive quantities of actin cables and actin cortical patches, as well as morphological aberrations (38).

The *oye2* and the DKO *oye2 oye3* strains used in the current study were in the BY4741 genetic background. Cells exhibited very mild cytoskeletal changes showing more intensely stained cortical patches, but not increased actin cables. However, the *Δoye2 glr1* strain exhibited an exacerbated phenotype which was very similar to the *act1-123* mutant, not only confirming the participation of the *oye2p* protein in actin polymerization, but also underscoring the importance of additional players participating, such as oxidized glutathione (Fig. 8). Actin cables are the tracks directing polarized cell secretion and organellar segregation. The actin filament bundles are anchored at one end to discrete regions in the cortex and radiate towards the rest of the cell (53). During cell division, in the process of nuclear positioning and segregation, actin was found to play a role in mitotic spindle orientation, as revealed in studies of actin gene mutations causing disruptions in nuclear orientation (54). The vacuole is also associated with actin cables, and specific alleles of the actin gene reduce the efficiency of vacuole inheritance (55).

Increased levels of glutathionylated proteins have been found in many human diseases such as Friedreich's ataxia, hyperlipidaemia, diabetes mellitus (56,57). S-glutathionylation offers the cell the advantage of a reversible mechanism that prevents the protein Cys thiol group from

irreversible oxidation. The effects seen in the case of the *Δoye2 glr1* cells clearly suggest the presence of an enzymatic mechanism that mediates glutathionylation of actin in the presence of high GSSG levels. In mammalian cells, a similar role in the catalysis of reversible protein thiol glutathionylation was recently assigned for glutaredoxin 2 (58).

The specific cooperative phenotype caused by the simultaneous deletion of *oye2* and *glr1* can be explained by the absence of the protective function of the *oye2p* on actin which renders cells with high levels of GSSG highly susceptible to actin glutathionylation, altering the polymerization dynamics. The effect seen is dependent on the presence of high levels of GSSG (Fig. 8), since the presence of increased ROS levels does not by itself cause the dramatic cytoskeletal rearrangements. The inactivation of *gsh1* with *oye2* although it led to high ROS levels and extreme sensitivity to oxidative stress, does not cause the characteristic morphology. In a previous study, we observed that when yeast cells were treated with the prooxidant CHP the total glutathione levels rose substantially compared to untreated cells. This was not the case for H₂O₂ treatment. Moreover, this GSH increase was dependent on the presence of the transcriptional activator Yap1 (59). Taken together, our data show that increased ROS do not automatically translate into depleted GSH levels, and that the presence of high GSSG is important on its own right

Evidence from several studies suggests crosstalk between the dynamics of the actin cytoskeleton, the release of ROS by mitochondria and RAS signaling, in controlling PCD in eukaryotic cells (60,61). The results shown further reinforce this model and place Old Yellow FMN-oxidoreductases in a center stage modulating oxidative stress and programmed cell death in a positive or negative manner, while *oye2p* together with GSH regulate actin dynamics and organelle segregation.

REFERENCES

1. Costerton, J. W., Stewart, P. S., and Greenberg, E. P. (1999) *Science* **284**(5418), 1318-1322
2. Cornillon, S., Foa, C., Davoust, J., Buonavista, N., Gross, J. D., and Golstein, P. (1994) *J Cell Sci* **107** (Pt 10), 2691-2704
3. Vachova, L., and Palkova, Z. (2005) *J Cell Biol* **169**(5), 711-717
4. Sinclair, D. A., Mills, K., and Guarente, L. (1998) *Trends Biochem Sci* **23**(4), 131-134

5. Ludovico, P., Sousa, M. J., Silva, M. T., Leao, C., and Corte-Real, M. (2001) *Microbiology* **147**(Pt 9), 2409-2415
6. Madeo, F., Frohlich, E., Ligr, M., Grey, M., Sigrist, S. J., Wolf, D. H., and Frohlich, K. U. (1999) *J Cell Biol* **145**(4), 757-767
7. Del Carratore, R., Della Croce, C., Simili, M., Taccini, E., Scavuzzo, M., and Sbrana, S. (2002) *Mutat Res* **513**(1-2), 183-191
8. Severin, F. F., and Hyman, A. A. (2002) *Curr Biol* **12**(7), R233-235
9. Herker, E., Jungwirth, H., Lehmann, K. A., Maldener, C., Frohlich, K. U., Wissing, S., Buttner, S., Fehr, M., Sigrist, S., and Madeo, F. (2004) *J Cell Biol* **164**(4), 501-507
10. Latterich, M., Frohlich, K. U., and Schekman, R. (1995) *Cell* **82**(6), 885-893
11. Ahn, S. H., Cheung, W. L., Hsu, J. Y., Diaz, R. L., Smith, M. M., and Allis, C. D. (2005) *Cell* **120**(1), 25-36
12. Madeo, F., Frohlich, E., and Frohlich, K. U. (1997) *J Cell Biol* **139**(3), 729-734
13. Shirogane, T., Fukada, T., Muller, J. M., Shima, D. T., Hibi, M., and Hirano, T. (1999) *Immunity* **11**(6), 709-719
14. Madeo, F., Herker, E., Maldener, C., Wissing, S., Lachelt, S., Herlan, M., Fehr, M., Lauber, K., Sigrist, S. J., Wesselborg, S., and Frohlich, K. U. (2002) *Mol Cell* **9**(4), 911-917
15. Fahrenkrog, B., Sauder, U., and Aebi, U. (2004) *J Cell Sci* **117**(Pt 1), 115-126
16. Wissing, S., Ludovico, P., Herker, E., Buttner, S., Engelhardt, S. M., Decker, T., Link, A., Proksch, A., Rodrigues, F., Corte-Real, M., Frohlich, K. U., Manns, J., Cande, C., Sigrist, S. J., Kroemer, G., and Madeo, F. (2004) *J Cell Biol* **166**(7), 969-974
17. Li, W., Sun, L., Liang, Q., Wang, J., Mo, W., and Zhou, B. (2006) *Mol Biol Cell* **17**(4), 1802-1811
18. Kane, D. J., Sarafian, T. A., Anton, R., Hahn, H., Gralla, E. B., Valentine, J. S., Ord, T., and Bredesen, D. E. (1993) *Science* **262**(5137), 1274-1277
19. Gross, A., Pilcher, K., Blachly-Dyson, E., Basso, E., Jockel, J., Bassik, M. C., Korsmeyer, S. J., and Forte, M. (2000) *Mol Cell Biol* **20**(9), 3125-3136
20. Jin, C., and Reed, J. C. (2002) *Nat Rev Mol Cell Biol* **3**(6), 453-459
21. Chae, H. J., Kim, H. R., Xu, C., Bailly-Maitre, B., Krajewska, M., Krajewski, S., Banares, S., Cui, J., Digicaylioglu, M., Ke, N., Kitada, S., Monosov, E., Thomas, M., Kress, C. L., Babendure, J. R., Tsien, R. Y., Lipton, S. A., and Reed, J. C. (2004) *Mol Cell* **15**(3), 355-366
22. Kampranis, S. C., Damianova, R., Atallah, M., Toby, G., Kondi, G., Tsihchlis, P. N., and Makris, A. M. (2000) *J Biol Chem* **275**(38), 29207-29216
23. Moon, H., Baek, D., Lee, B., Prasad, D. T., Lee, S. Y., Cho, M. J., Lim, C. O., Choi, M. S., Bahk, J., Kim, M. O., Hong, J. C., and Yun, D. J. (2002) *Biochem Biophys Res Commun* **290**(1), 457-462
24. Sawada, M., Sun, W., Hayes, P., Leskov, K., Boothman, D. A., and Matsuyama, S. (2003) *Nat Cell Biol* **5**(4), 320-329
25. Belhocine, S., Mbithe, C., Dimitrova, I., Kampranis, S. C., and Makris, A. M. (2004) *Cell Death Differ* **11**(8), 946-948
26. Stott, K., Saito, K., Thiele, D. J., and Massey, V. (1993) *J Biol Chem* **268**(9), 6097-6106
27. Reekmans, R., De Smet, K., Chen, C., Van Hummelen, P., and Contreras, R. (2005) *FEMS Yeast Res* **5**(8), 711-725
28. Westermann, B., and Neupert, W. (2000) *Yeast* **16**(15), 1421-1427
29. Gueldener, U., Heinisch, J., Koehler, G. J., Voss, D., and Hegemann, J. H. (2002) *Nucleic Acids Res* **30**(6), e23
30. Braun, R. J., Zischka, H., Madeo, F., Eisenberg, T., Wissing, S., Buttner, S., Engelhardt, S. M., Buringer, D., and Ueffing, M. (2006) *J Biol Chem* **281**(35), 25757-25767
31. Griffith, O. W. (1980) *Anal Biochem* **106**(1), 207-212

32. Bellot, G., Cartron, P. F., Er, E., Oliver, L., Juin, P., Armstrong, L. C., Bornstein, P., Mihara, K., Manon, S., and Vallette, F. M. (2006) *Cell Death Differ*
33. Dimitrova, I., Toby, G. G., Tili, E., Strich, R., Kampranis, S. C., and Makris, A. M. (2004) *FEBS Lett* **566**(1-3), 100-104
34. Kohli, R. M., and Massey, V. (1998) *J Biol Chem* **273**(49), 32763-32770
35. Collinson, L. P., and Dawes, I. W. (1995) *Gene* **156**(1), 123-127
36. Outten, C. E., and Culotta, V. C. (2004) *J Biol Chem* **279**(9), 7785-7791
37. Skulachev, V. P. (2001) *Trends Biochem Sci* **26**(1), 23-29
38. Haarer, B. K., and Amberg, D. C. (2004) *Mol Biol Cell* **15**(10), 4522-4531
39. Altmann, K., and Westermann, B. (2005) *Mol Biol Cell* **16**(11), 5410-5417
40. Karplus, P. A., Fox, K. M., and Massey, V. (1995) *Faseb J* **9**(15), 1518-1526
41. Sato, T., Hanada, M., Bodrug, S., Irie, S., Iwama, N., Boise, L.H., Thomson, C.B., Golemis, E., Fong, L., Wang, H. G., and Reed, J.C. (1994) *Proc. Natl. Acad. Sci USA* **94**(20), 9238-9242
42. Fox, K. M., and Karplus, P. A. (1994) *Structure* **2**(11), 1089-1105
43. Gavin, A. C., Aloy, P., Grandi, P., Krause, R., Boesche, M., Marzioch, M., Rau, C., Jensen, L. J., Bastuck, S., Dumpelfeld, B., Edelmann, A., Heurtier, M. A., Hoffman, V., Hoefert, C., Klein, K., Hudak, M., Michon, A. M., Schelder, M., Schirle, M., Remor, M., Rudi, T., Hooper, S., Bauer, A., Bouwmeester, T., Casari, G., Drewes, G., Neubauer, G., Rick, J. M., Kuster, B., Bork, P., Russell, R. B., and Superti-Furga, G. (2006) *Nature* **440**(7084), 631-636
44. Ho, Y., Gruhler, A., Heilbut, A., Bader, G. D., Moore, L., Adams, S. L., Millar, A., Taylor, P., Bennett, K., Boutilier, K., Yang, L., Wolting, C., Donaldson, I., Schandorff, S., Shewnarane, J., Vo, M., Taggart, J., Goudreault, M., Muskat, B., Alfarano, C., Dewar, D., Lin, Z., Michalickova, K., Willems, A. R., Sassi, H., Nielsen, P. A., Rasmussen, K. J., Andersen, J. R., Johansen, L. E., Hansen, L. H., Jespersen, H., Podtelejnikov, A., Nielsen, E., Crawford, J., Poulsen, V., Sorensen, B. D., Matthiesen, J., Hendrickson, R. C., Gleeson, F., Pawson, T., Moran, M. F., Durocher, D., Mann, M., Hogue, C. W., Figeys, D., and Tyers, M. (2002) *Nature* **415**(6868), 180-183
45. Krogan, N. J., Cagney, G., Yu, H., Zhong, G., Guo, X., Ignatchenko, A., Li, J., Pu, S., Datta, N., Tikuisis, A. P., Punna, T., Peregrin-Alvarez, J. M., Shales, M., Zhang, X., Davey, M., Robinson, M. D., Paccanaro, A., Bray, J. E., Sheung, A., Beattie, B., Richards, D. P., Canadian, V., Lalev, A., Mena, F., Wong, P., Starostine, A., Canete, M. M., Vlasblom, J., Wu, S., Orsi, C., Collins, S. R., Chandran, S., Haw, R., Rilstone, J. J., Gandi, K., Thompson, N. J., Musso, G., St Onge, P., Ghanny, S., Lam, M. H., Butland, G., Altaf-Ul, A. M., Kanaya, S., Shilatifard, A., O'Shea, E., Weissman, J. S., Ingles, C. J., Hughes, T. R., Parkinson, J., Gerstein, M., Wodak, S. J., Emili, A., and Greenblatt, J. F. (2006) *Nature* **440**(7084), 637-643
46. Zhu, H., Bilgin, M., Bangham, R., Hall, D., Casamayor, A., Bertone, P., Lan, N., Jansen, R., Bidlingmaier, S., Houfek, T., Mitchell, T., Miller, P., Dean, R. A., Gerstein, M., and Snyder, M. (2001) *Science* **293**(5537), 2101-2105
47. Muller, A., Hauer, B., and Rosche, B. (2007) *Biotechnol Bioeng* **98**(1), 22-29
48. Trotter, E. W., Collinson, E. J., Dawes, I. W., and Grant, C. M. (2006) *Appl Environ Microbiol* **72**(7), 4885-4892
49. Gasch, A. P., Spellman, P. T., Kao, C. M., Carmel-Harel, O., Eisen, M. B., Storz, G., Botstein, D., and Brown, P. O. (2000) *Mol Biol Cell* **11**(12), 4241-4257
50. Segal, E., Shapira, M., Regev, A., Pe'er, D., Botstein, D., Koller, D., and Friedman, N. (2003) *Nat Genet* **34**(2), 166-176
51. Grant, C. M., MacIver, F. H., and Dawes, I. W. (1997) *FEBS Lett* **410**(2-3), 219-222
52. Wang, J., Boja, E. S., Tan, W., Tekle, E., Fales, H. M., English, S., Mieyal, J. J., and Chock, P. B. (2001) *J Biol Chem* **276**(51), 47763-47766

53. Pruyne, D., Legesse-Miller, A., Gao, L., Dong, Y., and Bretscher, A. (2004) *Annu Rev Cell Dev Biol* **20**, 559-591
54. Palmer, R. E., Sullivan, D. S., Huffaker, T., and Koshland, D. (1992) *J Cell Biol* **119**(3), 583-593
55. Hill, K. L., Catlett, N. L., and Weisman, L. S. (1996) *J Cell Biol* **135**(6 Pt 1), 1535-1549
56. Niwa, T., Naito, C., Mawjood, A. H., and Imai, K. (2000) *Clin Chem* **46**(1), 82-88
57. Pastore, A., Tozzi, G., Gaeta, L. M., Bertini, E., Serafini, V., Di Cesare, S., Bonetto, V., Casoni, F., Carrozzo, R., Federici, G., and Piemonte, F. (2003) *J Biol Chem* **278**(43), 42588-42595
58. Beer, S. M., Taylor, E. R., Brown, S. E., Dahm, C. C., Costa, N. J., Runswick, M. J., and Murphy, M. P. (2004) *J Biol Chem* **279**(46), 47939-47951
59. Kilili, K. G., Atanassova, N., Vardanyan, A., Clatot, N., Al-Sabarna, K., Kanellopoulos, P. N., Makris, A. M., and Kampranis, S. C. (2004) *J Biol Chem* **279**(23), 24540-24551
60. Gourlay, C. W., Carpp, L. N., Timpson, P., Winder, S. J., and Ayscough, K. R. (2004) *J Cell Biol* **164**(6), 803-809
61. Breitenbach, M., Laun, P., and Gimona, M. (2005) *Trends Cell Biol* **15**(12), 637-639

Acknowledgements

O.O, S.M. & H.K were partially supported by CIHEAM/MAICh student scholarships. We thank Erica Golemis for useful comments on the manuscript and Mohamed El-Sayed for his graphic art help.

Abbreviations

The abbreviations used are: ROS, reactive oxygen species; PCD, programmed cell death; OYE, old yellow enzyme; GSH, γ -glutamylcystinylglycine; GSSG, glutathione disulfide; CM, complete medium; *t*-BOOH, tert-butyl hydroperoxide; CHP, cumene hydroperoxide; FMN, flavin mononucleotide; HE, hydroethidium; DKO, double knockout; EMS, ethane methyl sulfonate; Glu, glucose; mit-GFP, mitochondria targeted green fluorescent protein.

Figure Legends

Figure 1. The C-terminus OYE2 restores Bax sensitivity and proper targeting of mit-GFP to the mitochondria in R13 yeast mutants. (A) EGY48 wt cells expressing Bax and empty vector (Bax lethal, control), R13 EMS mutant cells co-expressing Bax with (314-400) OYE2 or Tvl-1 as negative control, were plated on gal raff/CM-his, trp to induce protein expression. (B) Expression of (314-400) OYE2 fusion protein was detected using anti-HA antibodies in a western blot. (C, top row) Left, wild type EGY48 cells expressing mitochondria targeted GFP (mit-GFP); center, R13- yeast cells fail to properly target mit-GFP to mitochondria; right, R13 cells co-expressing the (314-400) OYE2 clone (C-term. OYE2) are restored in proper mit-GFP targeting. (C, middle row) Left, EGY48 wt cells expressing Bax exhibit a heterogeneous population of cells with swollen or fragmented mitochondria (stained with mitotracker); center, expression of Bax in R13 mutant cells has no effect in mit-GFP targeting; right, (314-400) OYE2 restores mit-GFP targeting in the presence of Bax in the R13 mutant cells. (C bottom row), Right, YFP-Bax fusion localizes on mitochondria in wt EGY48 cells; middle, YFP shows diffuse fluorescence when expressed in EGY48 cells; left, YFP-Bax fails to localize on mitochondria in R13 mutant cells. The cell outlines are delineated by red fluorescence.

Figure 2. Expression of full length OYE2 suppresses Bax lethality. (A) EGY48 cells co-expressing Bax with full length OYE2, C-term. (314-400) OYE2 or empty vector, are plated in gal-raff/CM-his, trp. (B) Left, mitochondria of wild type EGY48 cells expressing Bax stained with mitotracker green;

right, co-expression of Bax with full length OYE2 in wild type EGY48 cells restores mitochondrial morphology.

(C) EGY48 wild type cells expressing an OYE2-GFP fusion, under the control of a galactose promoter, were stained with mitotracker red CMXRos. The same cell was examined for GFP fluorescence and mitochondrial staining. Bright yellow stain identifies areas of overlapping fluorescence.

Figure 3. Reactive oxygen species levels in, +OYE2, +OYE3, $\Delta oye2$, $\Delta oye3$ cells treated with prooxidants. (A) Wild type BY4741 cells, BY4741 cells overexpressing OYE2 or OYE3 and the deletion mutants $\Delta oye2$ and $\Delta oye3$ were treated with 1.5 mM H₂O₂, 1 mM *t*-BOOH, 0.2 mM CHP for 1 hour or were left untreated. ROS levels were measured by HE staining and were analysed by FACS. (B) Wild type BY4741 cells and the deletion mutants $\Delta sod1$ and $\Delta ctt1$ were treated with 1.5mM H₂O₂ for 1 hour or left untreated. ROS levels were measured as above. BY4741 wt cells are shown in vertical lines in all graphs. The mean percentage changes of fluorescent intensities of cells compared to identically treated wt cells are shown.

Figure 4. OYE2 and OYE3 modulate H₂O₂-induced PCD. (A) BY4741 wt cells overexpressing OYE2 or OYE3 in moderate levels from a constitutive TPI promoter, or harboring an empty vector were resuspended in equal densities in fresh glu/CM-leu media and 2 hours later H₂O₂ was added at 1.5 mM final concentration. The cell cultures were evaluated for their capacity to recover by monitoring OD₆₀₀ at regular intervals; (B) BY4741 wt cells overexpressing a C-terminal truncation of OYE2 (1-388) OYE2 recover faster than OYE2 overexpressing cells; (C) logarithmically grown cells were resuspended in fresh medium at the same OD₆₀₀. Equal volume aliquots were used to inoculate fresh media at very low density which were subsequently treated with 1 mM H₂O₂ for 2 hours. Viable cells were enumerated, prior and post treatment, by plating serial dilutions on YPD plates. (D) OYE3 overexpressed in $\Delta oye2$ cells is compared to $\Delta oye2$ cells harboring empty vector and wild type cells overexpressing OYE3 in the growth recovery assay described above; (E) $\Delta oye3$ cells overexpressing OYE2, (1-388) OYE2 or empty vector were monitored for growth recovery subsequent to H₂O₂ insult. The OYE2 truncated form exerts no protection in the absence of OYE3. (F) BY4741 wt cells overexpressing OYE2, Y197F OYE2 or empty vector were monitored for growth recovery subsequent to H₂O₂ insult. (G) $\Delta oye3$ cells overexpressing OYE2, Y197F OYE2 or empty vector were monitored for growth recovery as above. (H) Western blot detection of *oye2p* and its corresponding mutants Y197F and (1-388) C-terminal truncation using anti-HA antibodies.

Figure 5. The double knockout $\Delta oye2 oye3$ cells are highly resistant to H₂O₂-induced PCD, cell death during adaptive regrowth, and exhibit upregulated respiratory capacity. BY4741 wild type parental cells (-◆-), $\Delta oye2$ (-□-), $\Delta oye3$ (-▲-) and $\Delta oye2 oye3$ (-×-) cells were used in the following assays. (A) Fresh cells were resuspended at equal densities in fresh glu/CM media and 2 hours later H₂O₂ was added at 1.5 mM final concentration. The cell cultures were evaluated for their capacity to recover by monitoring OD₆₀₀ at regular intervals. (B) Logarithmically growing cells were resuspended at the same OD₆₀₀ in fresh medium. Equal volume aliquots were used to inoculate fresh media at very low density which were subsequently treated with 1 mM H₂O₂ for 2 hours. Viable cells were enumerated, prior and post treatment, by plating serial dilutions on YPD plates. (C) $\Delta yca1$ cells (-◇-) $\Delta oye2 oye3$ and wt cells were treated with 0.8mM H₂O₂ and their capacity to recover was monitored as above. $\Delta oye2 oye3$ cells recover faster compared to $\Delta yca1$ cells. (D) Annexin V staining of externalized PS in $\Delta oye2 oye3$ treated with H₂O₂ (E) ROS levels of $\Delta oye2 oye3$ were compared to BY4741 wild type cells (in vertical lines) were measured by HE staining and were analyzed by FACS. (F) Overexpression of OYE2 (-□-), OYE3 (-▲-), (1-388) OYE2 (-×-) in $\Delta oye2 oye3$ cells does not confer any additional protection as compared to the double knockout strain harboring empty vector (-

◆-). (G) Fresh overnight cultures of the above strains and EGY48 wild type cells (which respire efficiently), were washed twice with H₂O, 5-fold serially diluted and spotted on glucose based (YPD) and glycerol based (YPG) rich media. (H) *Δoye2 oye3* cells ρ⁰ cells were generated by ethidium bromide treatment. Five strains (A-E) isolated from treated cells and the parental *Δoye2 oye3* strain, were plated in YPD and YPG plates as above. (I) BY4741 wild type cells, the parental *Δoye2 oye3* strain and 3 ρ⁰ *Δoye2 oye3* (A-C) strains were treated by H₂O₂ pulse as in 6B and enumerated by plating serial dilutions on YPD plates. The ρ⁰ strains are sensitive to H₂O₂-induced PCD. (J) Fully saturated cultures grown in 2% glucose CM media were allowed to age chronologically. Cell viability was measured by plating serial dilutions at regular intervals. (K) Aliquots of fresh cells grown as above, diluted in fresh glucose CM were treated with 10 mM, 20 mM, 40 mM of acetic acid for 2 hours. Viable cells were enumerated prior and post treatment as above.

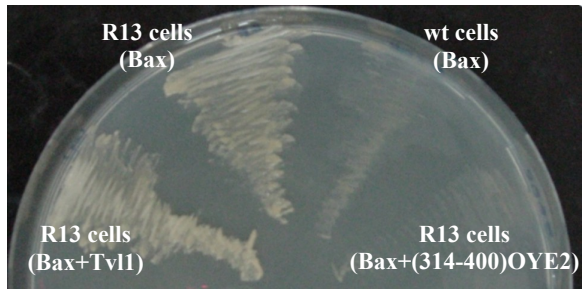
Figure 6. Double deletions of *oye2* with antioxidant genes significantly enhance ROS levels and H₂O₂-induced PCD. Endogenous levels of ROS were measured by FACS in: (A) *Δsod1* vs. its respective double deletion with *oye2*, *Δoye2 sod1*; (C) *Δctt1* vs. *Δoye2 ctt1*; (D) BY4741 wt cells vs. *Δyca1*; (E) *Δyca1* vs. *Δoye2 yca1*; (G) BY4741 wt cells vs. *Δglr1*; (H) *Δglr1* vs. *Δoye2 glr1* cells. Wild type cells are always shown in vertical lines. In the graphs where single mutants are compared to their double knockout counterparts, the former are always shown in vertical lines. The ability of cells to resist H₂O₂-induced PCD was examined for *Δsod1* (-□-), *Δoye2 sod1* (-△-), and wt cells (-◆-) shown in (B); for *Δyca1* (-■-), *Δoye2 yca1* (-×-), and wt cells (-◆-) shown in (F); for *Δglr1* (-○-), *Δoye2 glr1* (-●-) and wt cells (-◆-) shown in (J). All cells were treated with 1.25 mM H₂O₂ and assayed for growth recovery. Mitochondria in *Δoye2 glr1* cells which were visualized by a mit-GFP exhibit thinner tubules and signs of fragmentation (I).

Figure 7. *Δoye2 glr1* cells show dramatic alterations in cell morphology, the cytoskeleton, and organelle partition. The strains BY4741 wt, *Δoye2*, *Δglr1* and their DKO *Δoye2 glr1* were stained with Evans blue and photographed at 400X (left column); the actin cytoskeleton was visualized by staining with rhodamine-phalloidin (second column); nuclei were stained with Hoechst 33342 (third column) and the vacuolar lumen was stained with CMAC (right column)

Figure 8. Supplementation of *Δoye2 glr1* cells with exogenous GSH restores normal cell morphology. *Δoye2 gsh1* cells exhibit substantially higher levels of ROS than *Δgsh1* cells (in vertical lines) (top left). The cells even though are unable to synthesize GSH and are very sensitive to stress, they maintain normal morphology (top right). *Δoye2glr1* cells revert back to normal cell morphology when the medium was supplemented with 5 mM GSH (middle row). *Δoye2glr1* exhibit a dramatic 6pfold increase in GSSG levels (bottom row).

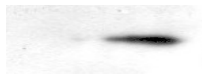
Figure 9. Model of OYE2 action. Oye2p homodimers preserve cell viability from oxidative damage by neutralizing generated ROS from mitochondria, and protect C285, C374 in actin from oxidation. In the absence of OYE2, high levels of oxidized glutathione (GSSG) attack and glutathionylate the two cysteines altering the polymerization dynamics. The oye2p-oye3p heterodimers on the other hand, sensitize cells to oxidative damage and enhance PCD in yeast.

A



(314-400) OYE2

- +



B

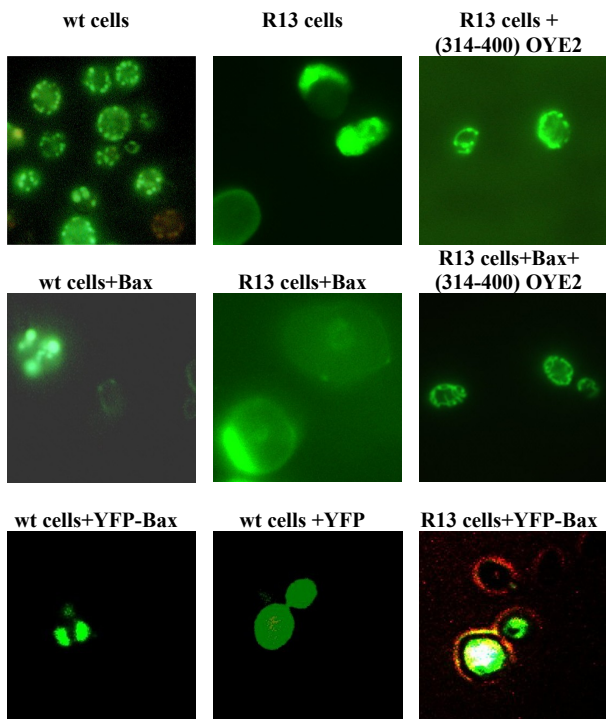
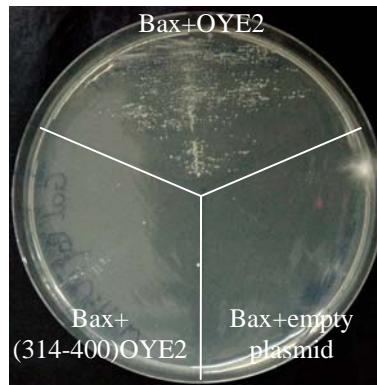
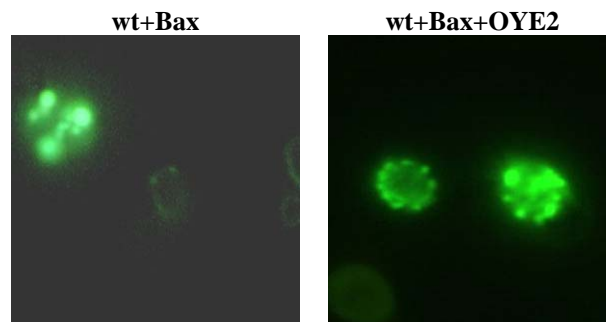


Figure 1 - Odat et al.

A



B



C

Mit. red + OYE2-GFP



Figure 2 – Odat et al.

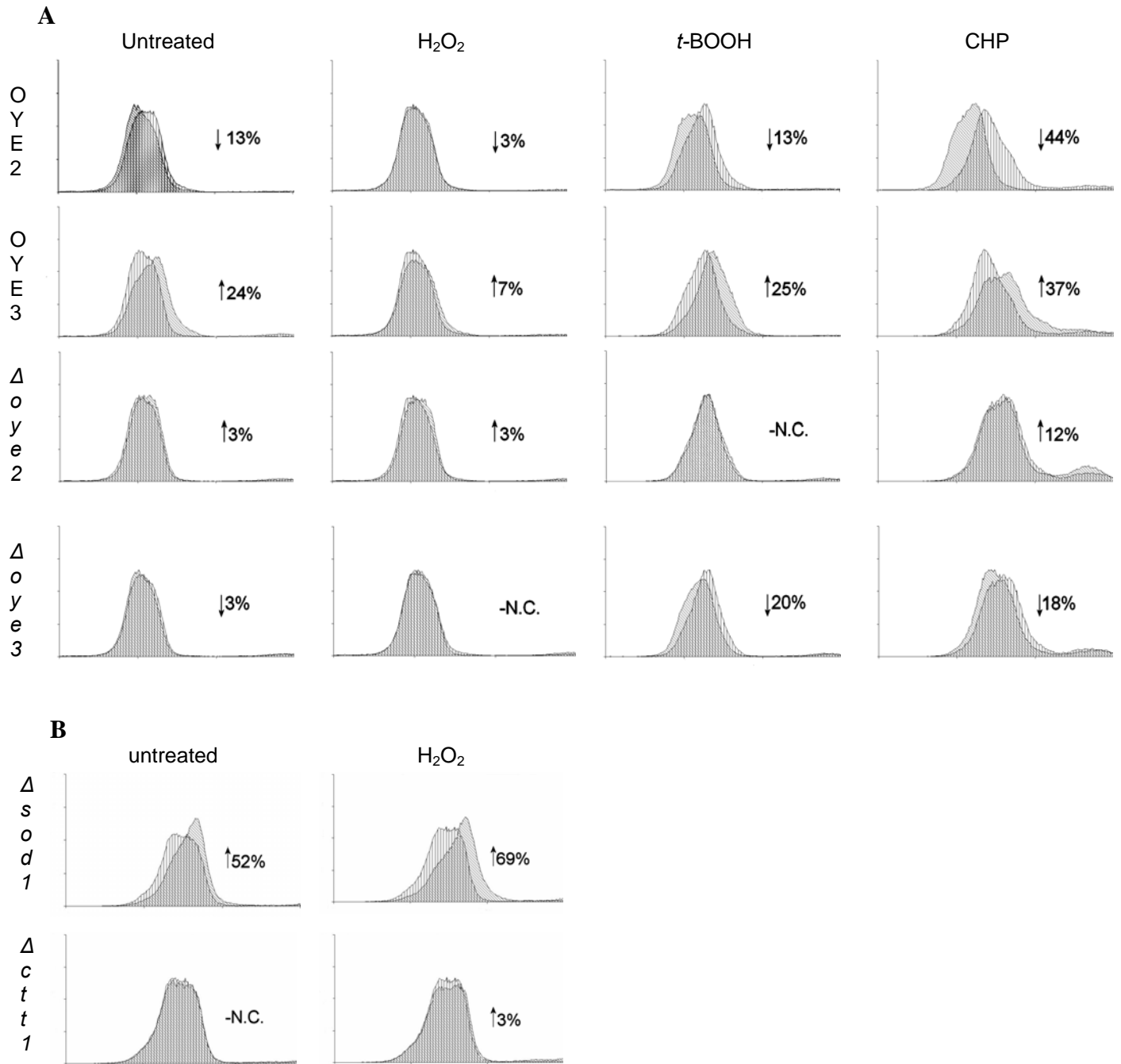


Figure 3- Odat et al.

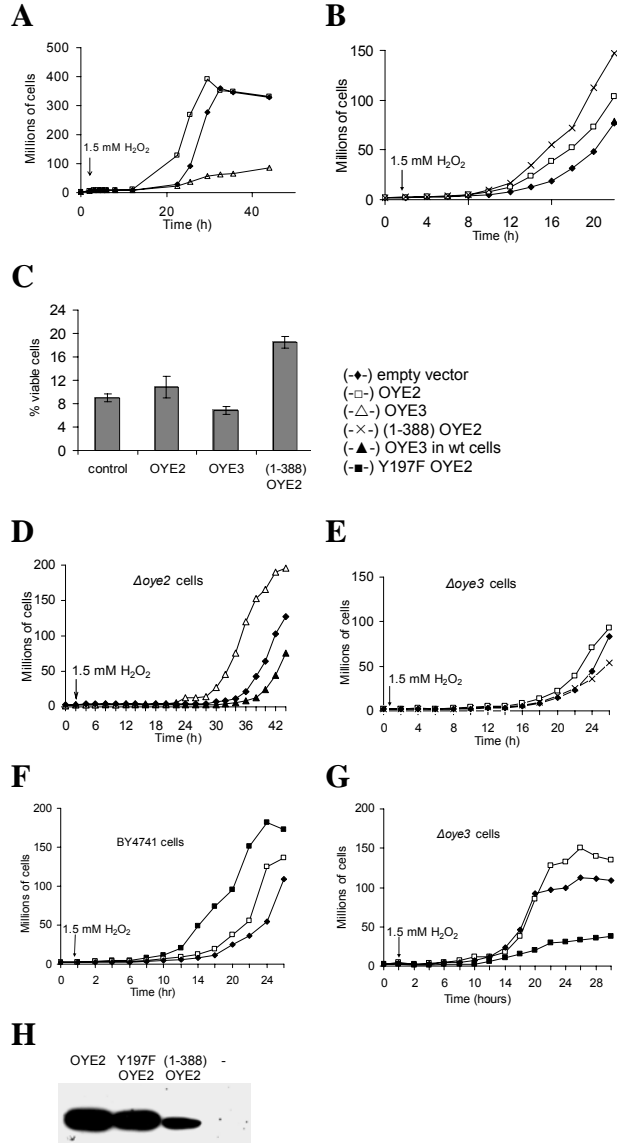


Figure 4-Odat et al.

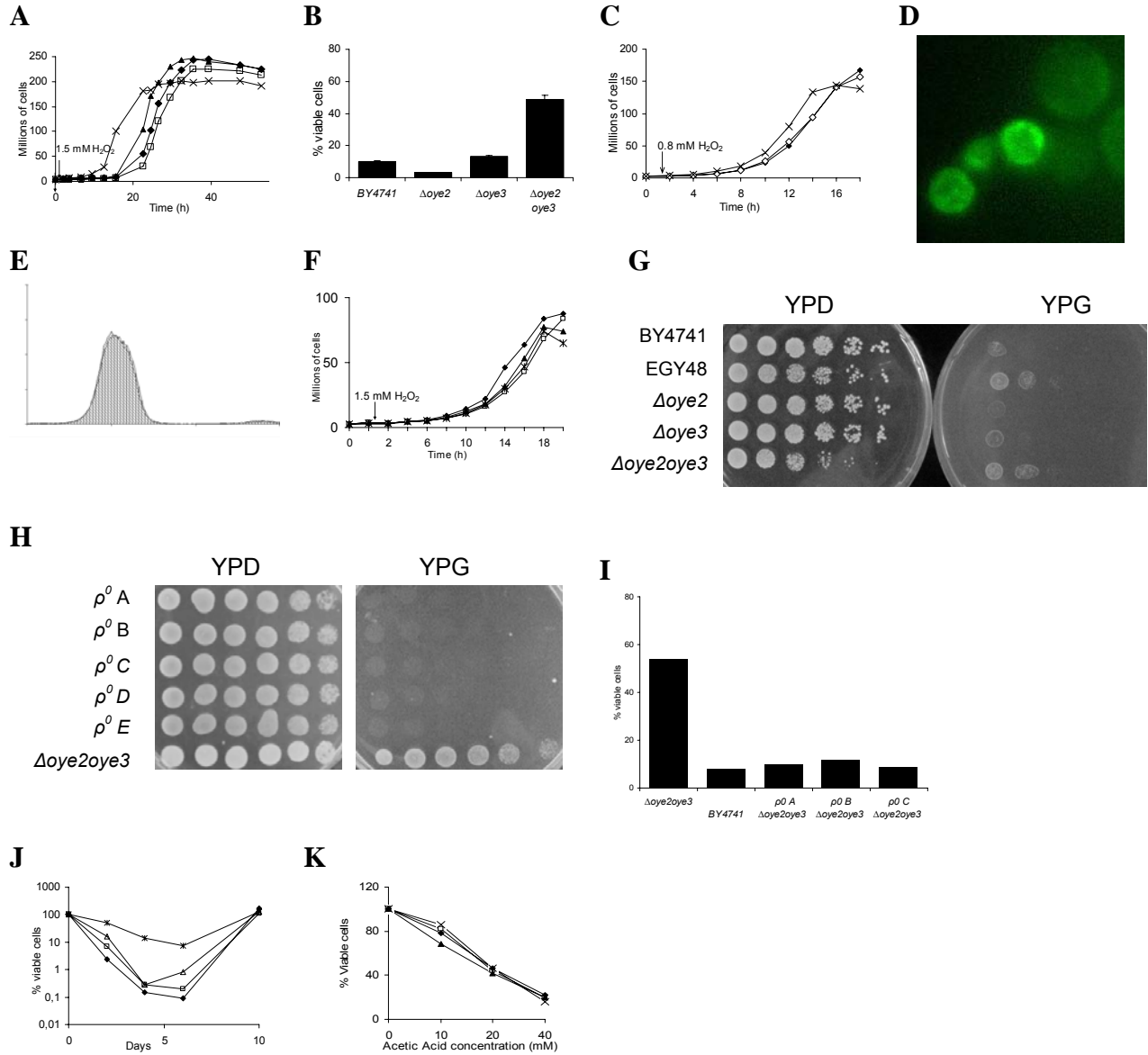


Figure 5- Odat et al.

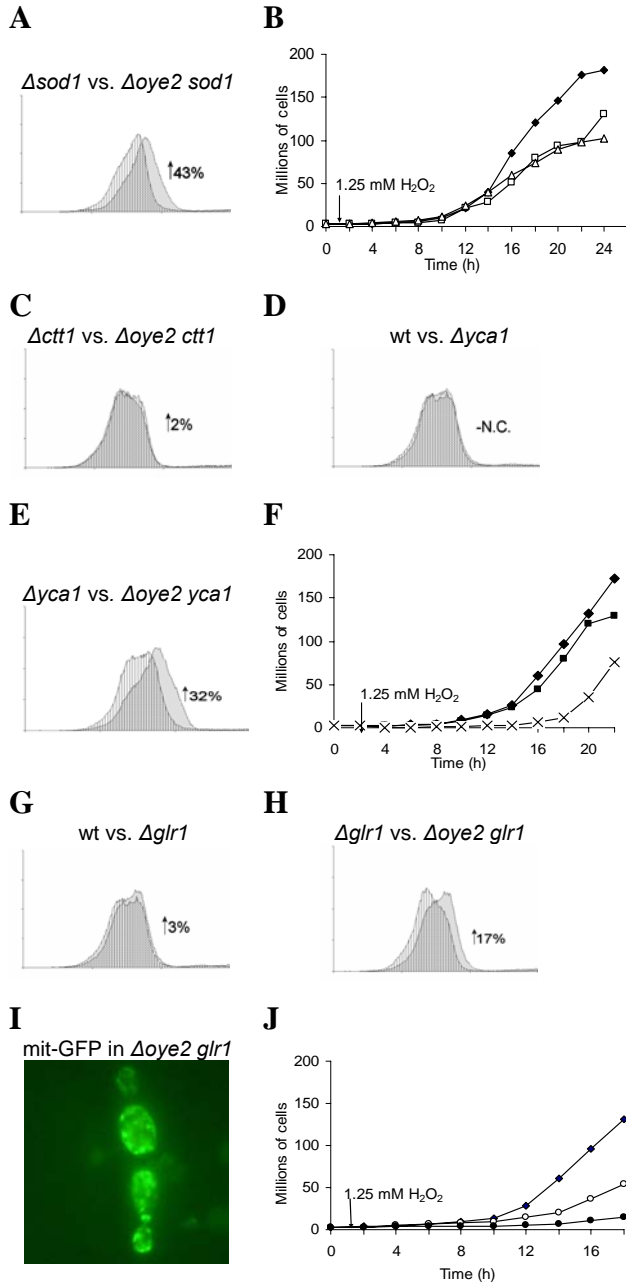


Figure 6-Odat et al.

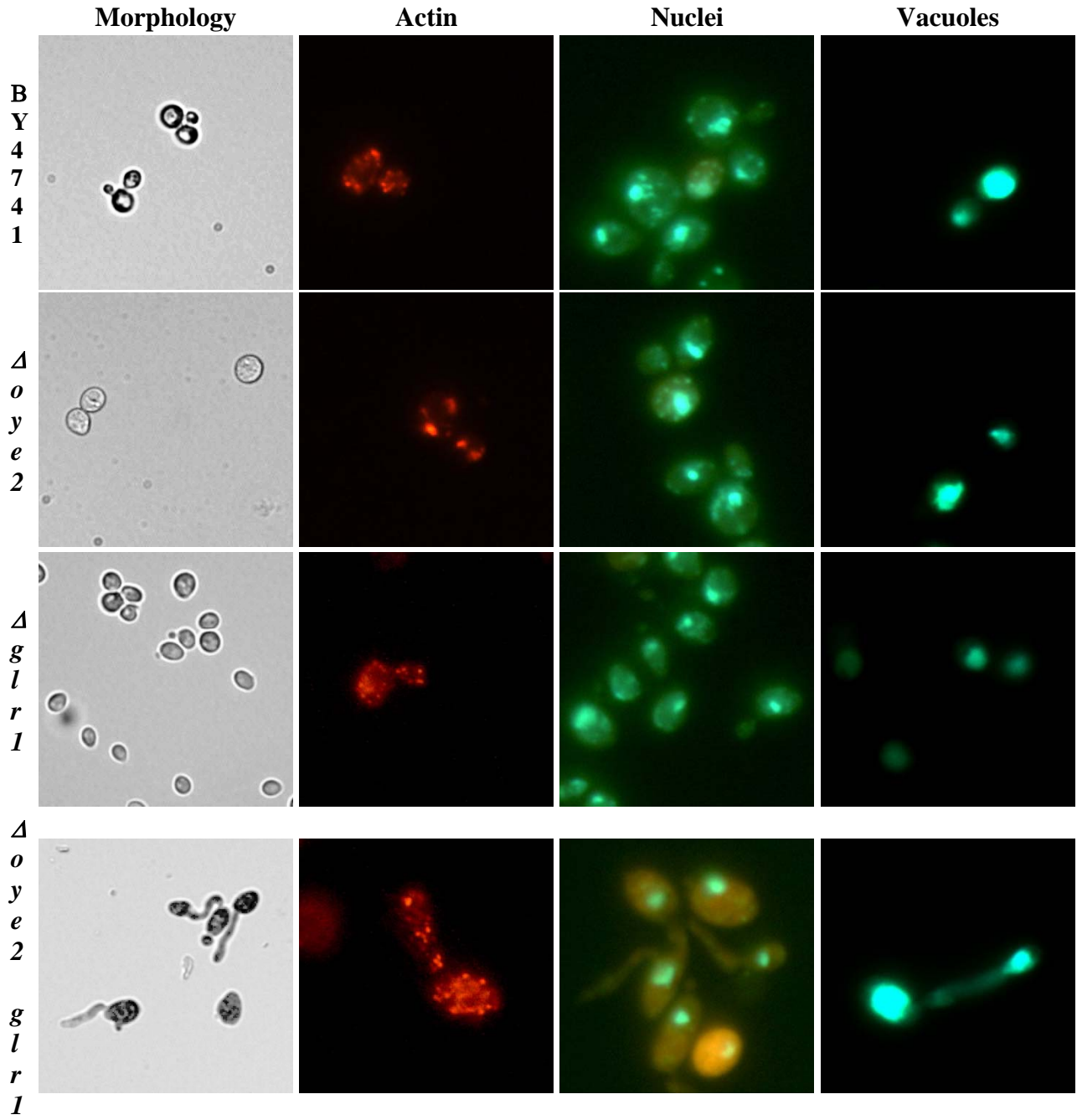
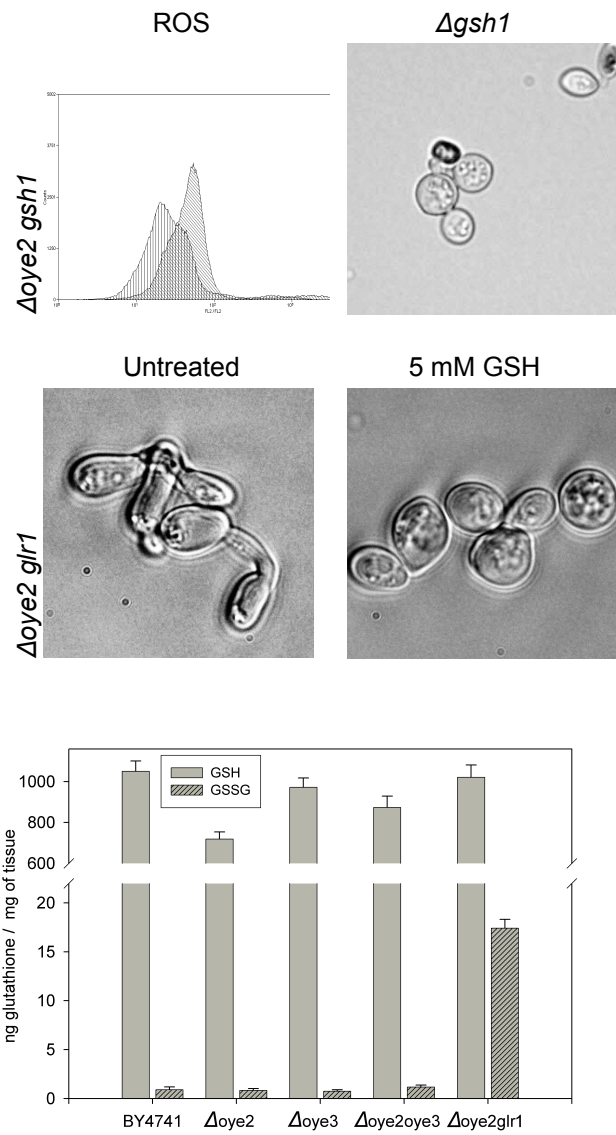


Figure 7 - Odat et al.



Odat et al. Figure 8

